Experimental Demonstration of Optical Packet Switching in Quantum Wrapper Networks

Mehmet Berkay On(1), Sandeep Kumar Singh(1), Gamze Gül(2)
Gregory S. Kanter(2), Roberto Proietti(3), Prem Kumar(2), S. J. Ben Yoo(1)

(1) University of California, Davis, CA, 95616, USA sbyoo@ucdavis.edu
(2) Northwestern University, Evanston, IL 60208, USA
(3) Politecnico di Torino, Turin, 10141, Italy

Abstract *We experimentally demonstrate optical packet switching for quantum payloads and classical burst headers in a three-node quantum wrapper network. Further, we record coincidence count distributions of polarization-entangled photon pairs between the source node and two distinct destination nodes and measure the coincidence-to-accidental ratio above 6.02.*

Introduction

A quantum network is an essential step for the future quantum internet that aims to establish quantum communication links between a large number of users[1]. Quantum networks will be necessary to distribute entanglement across these links to remote quantum devices[2],[3]. However, quantum bits (qubits) vary significantly from classical bits. They cannot be copied, amplified, or monitored[2],[4]. These properties make quantum networks appropriate for applications such as secure communication, quantum teleportation, and distributed quantum computing[1],[5],[6]. At the same time, they also lead to challenging requirements for developing quantum devices and protocols that are already available in classical networks for buffering, amplification, routing, transport control, and network management[7].

In recent years, there have been various efforts to develop quantum devices, protocols, and experimental testbeds for efficient quantum networks such as on-demand entanglement delivery[8], routing entanglement[9], quantum memories[10],[11], and distributed quantum computing[12]. Moreover, the possibility of using the existing fiber-optic infrastructure instead of dark fibers has been studied for quantum key distribution (QKD)[13]–[15] and entanglement distribution[9],[16]. However, managing a quantum network coexisting with today's classical networks remains a challenge. Therefore, quantum networks need a strategy to transport qubits with some level of performance guarantee in *Quality of Transmission* (QoT) and *Quality of Entanglement (QoE)* while switching or routing without damaging the qubits[17]. They also must be adaptable to new technologies in quantum devices such as quantum repeaters, memories as well as traditional classical network protocols such as the Transport Control Protocol over Internet Protocol (TCP/IP)[18].

Quantum Wrapper Networking (QWN) is such a new technology for quantum networks, which is inspired by Optical Label Switching (OLS)[19]. It utilizes the current networking platform with backward compatibility, transparency and interoperability as discussed in[18]. Quantum information packages in a QWN, in other words, quantum wrapper (QW) datagrams, are qubits wrapped with classical QW header (optionally QW tail) bits. QW datagrams can carry information about the quantum payload, the destination, and timing to coordinate end-to-end transmission without touching the quantum data. QW headers also help monitor the communication channel as we previously showed using the correlation between bit-error-rate (BER) of QW headers and the coincidence-to-accidental-coincidence ratio (CAR) of quantum payloads[20].

In this paper, we experimentally demonstrate quantum payload switching in a three-node quantum wrapper network with one source node, two distinct destination nodes, and one switching node between them. The switching node reads the QW header and routes the QW datagrams to their destinations without disturbing the qubits payload. We also demonstrate the QW header swapping functionality at the switching node, where a newly generated QW header replaces the old header and wraps the delayed quantum payload again, as shown in Fig. 1. As in an multi-purpose label switching networks, this type of QW header swapping mechanisms can offer scalability of a label switched network

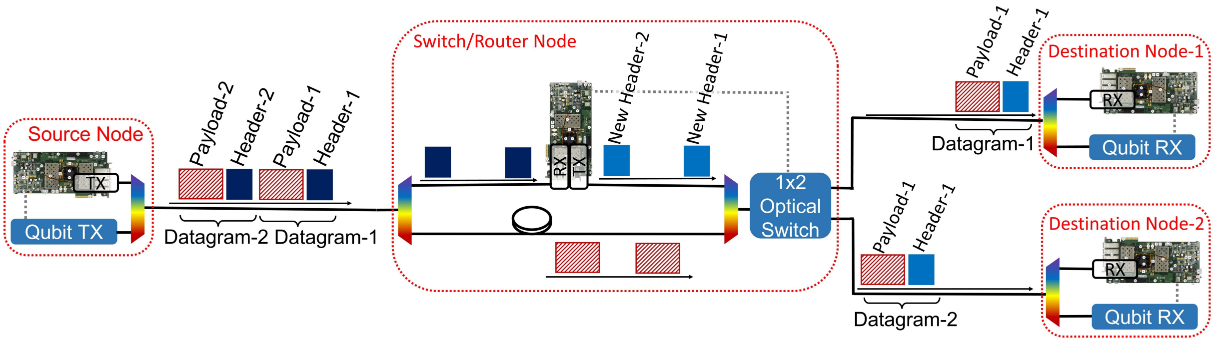

Fig. 1: A schematic of quantum payload switching by reading classical headers in a quantum wrapper network, which consists of a source node, two distinct destination nodes, and a switch/router node between the source and two destination nodes.

beyond the number of QW headers available[21]. We used field-programmable gate array (FPGA) boards to (re)generate QW headers, as well as to synchronize QW datagrams. Further, the classical header receivers at the destination nodes are synchronized with the quantum receivers and precisely gate the coincidence count measurement during the payload duration. Our experimental results show that the coincidence-to-accidental ratio is more than 6.02 for all scenarios in the QWN testbed, while the header bit-error rates (BER) are below 10^{-11}.

Experimental Setup and Results

Fig. 2 shows the experimental setup. We use a periodically poled silica-fiber-based polarization-entangled photon source (EPS-1000 from OZ Optics). The EPS is continuously pumped and generates entangled pairs centered around 1565.72 nm with >80 nm bandwidth. A thin film coating-based demultiplexer (single-mode MWDM from AC Photonics) separates entangled photon pairs, *signal* and *idler* in the wavelength channels 1570-1610 nm and 1500-1563 nm respectively. We use dense WDM pluggable transceivers at 1561.41 nm on an FPGA board (Xilinx Virtex-7 series VC709) to transmit and receive classical headers. A header consists of a clock-data-recovery (CDR) pilot sequence, a header start and data align sequence, a payload destination sequence, a payload duration sequence, a pseudo-random bit sequence (PRBS-11), and a header stop sequence. The total header duration is 41.28 μs at 10 Gb/s data rate. We assign 165.12 μs for the quantum packets. During the each quantum payload, the classical header transmitter (TX) is powered off by the FPGA logic circuit to avoid any crosstalk. In this experiment, QW datagrams are transmitted to the destination nodes one by one repetitively.

The implemented switch/router has two main functionalities: header swapping and optical QW datagram switching. The header swapper analyzes header bits and reconfigures the optical switch immediately after identifying the payload destination sequence. Additionally, a dedicated DWDM TX at 1561.41 nm in the switch/router node generates new headers. Commercial pluggable receivers (RX) typically have >5 μs CDR locking time[22]. To avoid delaying quantum payloads in the range of μs, we implement an external "trigger" connection. We power-split the optical signal, where half of the power goes to the commercial RX, while an EDFA amplifies the other half which goes to an analog photodetector. The detected signal is filtered by an 11 MHz low-pass filter (LPF) and connected to FPGA board as a trigger signal, as seen in Fig. 2 (a). When the first bits of the header reach the header swapper RX, it enters the CDR locking cycle; meanwhile trigger signal goes "high". The TX in the header swapper module starts to generate the CDR pilot sequence of the new headers immediately. This way, we need to delay quantum payloads only for <400 ns by a 80 m fiber spool due to payload destination identification time and electrical circuit delay.

We use an Agiltron NanoSpeed 2x2 polarization insensitive optical switch with 50 ns fall/rise time and ~20 dB extinction ratio. Because only one pair of single photon detectors (SPD, LYNXEA-NIR InGaAs avalanche photodiodes from AureaTechnology) are available in the lab, we coupled two optical links after the switching by a wideband power coupler. The optical links, *destination-1* and *destination-2*, have different fiber lengths, 80 and 60 meters, respectively. Therefore, as shown in Fig. 3 (a), coincidence count peaks appear at different time offsets. We aligned three fiber polarization controllers (FPC), one FPC for *idler* and two FPC for the signal at both *destination-1* and *destination-2*. While *destination-2* and *idler* polarization axis are paral-

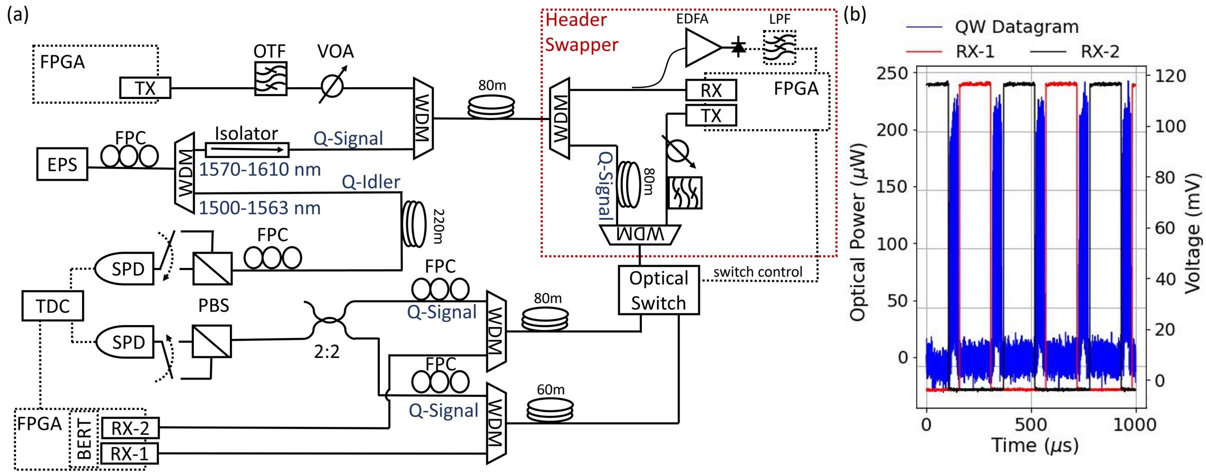

Fig. 2: (a) Detailed experimental setup, VOA: variable optical attenuator, OTF: optical tunable filter, PBS: polarization beam splitter, FPC: fiber-based polarization controller, BERT: bit-error-rate tester.(b) The blue trace is detected QW datagram on the scope, and the red and black traces are electrical signals that trigger the coincidence count measurements when high.

lel, we aligned *destination-1*'s axis as orthogonal to others. Therefore, the coincidence count peak around 166.5 ns is measured at the "HH" polarization basis when the peak around 70.5 ns is measured in "HV" basis as seen in the Fig. 3 (a).

After the headers reach their respective destination nodes, the payload duration is identified. The destination node RX generates an electrical gating signal connected to the SPDs to enable the coincidence count measurements. A time-to-digital converter circuit (TDC) is enabled after the header stop sequence is identified (plus a certain guard time) as long as the received payload duration information. Fig. 2 (b) shows the gating signals from *destination-1* and *destination-2* RXs. The SPDs operate at 20% quantum efficiency and 15 μs dead-time. The coincidence counts measurement time is 200 seconds which means thousands of quantum packets are aggregated to clearly observe the coincidence count distributions. We record coincidence-to-accidental ratio (CAR) values of 7.05 and 6.02 at *destination-1* and *destination-2*, respectively (where CAR = $\mathrm{CC}_{\max}/\mathrm{CC}_{\min}$). The CAR difference between the links may come from non-ideal polarization alignment and uneven link attenuation. During the measurements, the header bit-error-rates (BER) in the links between the source and switch nodes and the switch and destination nodes are below 10^{-11} for the received header power of -25 dBm.

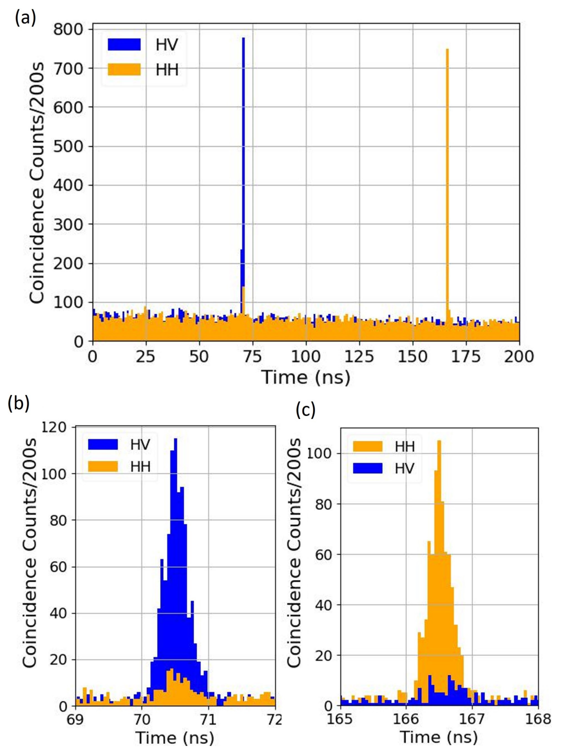

Fig. 3: Coincidence count histograms with polarization bases of "HH" ("H" *idler* and "H" *signal*) and "HV" ("H" *idler* and "V" *signal*), (a) bin size 1 ns, (b-c) bin size 50 ps

Conclusions

In this work, we implemented a three-node quantum wrapper network with two distinct destination nodes. We successfully demonstrated quantum payloads switching between the destination nodes by reading the classical headers at the switching node. Additionally, we synchronized SPDs with the received headers and gate the coincide count measurements only during the quantum payload time interval. The CAR is 6.02 and 7.05 for *source*-to-*destination-2* and *source*-to-*destination-1* respectively, when the header BERs are below 10^{-11} for all three links in the experimental setup. We plan to scale up the number of nodes and use longer links (in the range of several kilometers) in our future studies.

Acknowledgements

This work is supported by the U.S. DOE, Office of ASCR program under Award Number DE-SC-0022336.

References

[1] S. Wehner, D. Elkouss, and R. Hanson, "Quantum internet: A vision for the road ahead", *Science*, vol. 362, no. 6412, Oct. 2018, ISSN: 10959203. DOI: 10.1126/science.aam9288.

[2] H. J. Kimble, "The quantum internet", *Nature 2008 453:7198*, vol. 453, no. 7198, pp. 1023–1030, Jun. 2008, ISSN: 1476-4687. DOI: 10.1038/nature07127.

[3] C. Simon, "Towards a global quantum network", *Nature Photonics 2017 11:11*, vol. 11, no. 11, pp. 678–680, Oct. 2017, ISSN: 1749-4893. DOI: 10.1038/s41566-017-0032-0. arXiv: 1710.11585.

[4] W. K. Wootters and W. H. Zurek, "A single quantum cannot be cloned", *Nature 1982 299:5886*, no. 5886, pp. 802–803, ISSN: 1476-4687. DOI: 10.1038/299802a0.

[5] S. Hermans, M. Pompili, H. Beukers, S. Baier, J. Borregaard, and R. Hanson, "Qubit teleportation between non-neighbouring nodes in a quantum network", *Nature*, vol. 605, no. 7911, pp. 663–668, 2022.

[6] A. S. Cacciapuoti, M. Caleffi, F. Tafuri, F. S. Cataliotti, S. Gherardini, and G. Bianchi, "Quantum internet: Networking challenges in distributed quantum computing", *IEEE Network*, vol. 34, no. 1, pp. 137–143, 2019. DOI: 10.1109/MNET.001.1900092.

[7] S. Singh, M. On, R. Proietti, G. Kanter, P. Kumar, and S. Yoo, "Experimental demonstration of correlation between copropagating quantum and classical bits for quantum wrapper networking", *ECOC*, Sep. 2022.

[8] M. Pompili, C. Delle Donne, I. te Raa, *et al.*, "Experimental demonstration of entanglement delivery using a quantum network stack", *npj Quantum Information 2022 8:1*, vol. 8, no. 1, pp. 1–10, Oct. 2022, ISSN: 2056-6387. DOI: 10.1038/s41534-022-00631-2.

[9] M. Pant, H. Krovi, D. Towsley, *et al.*, "Routing entanglement in the quantum internet", *npj Quantum Information 2019 5:1*, vol. 5, no. 1, pp. 1–9, Mar. 2019, ISSN: 2056-6387. DOI: 10.1038/s41534-019-0139-x.

[10] M. K. Bhaskar, R. Riedinger, B. Machielse, *et al.*, "Experimental demonstration of memory-enhanced quantum communication", *Nature 2020 580:7801*, vol. 580, no. 7801, pp. 60–64, Mar. 2020, ISSN: 1476-4687. DOI: 10.1038/s41586-020-2103-5.

[11] J. V. Rakonjac, S. Grandi, S. Wengerowsky, D. Lago-Rivera, F. Appas, and H. de Riedmatten, *Transmission of light-matter entanglement over a metropolitan network*, 2023. arXiv: 2304.05416 [quant-ph].

[12] S. Bahrani, R. Wang, R. Oliveira, R. Nejabati, and D. Simeonidou, "Analysing the effect of quantum network interconnect on the performance of distributed quantum computing", in *Optical Fiber Communication Conference (OFC) 2023*, Optica Publishing Group, 2023, Tu2H.2.

[13] S. K. Joshi, D. Aktas, S. Wengerowsky, *et al.*, "A trusted node-free eight-user metropolitan quantum communication network", *Science Advances*, vol. 6, no. 36, Sep. 2020, ISSN: 23752548. DOI: 10.1126/sciadv.aba0959.

[14] J. Wang, B. J. Rollick, Z. Jia, H. Zhang, and B. A. Huberman, *Time-interleaving enabled co-propagation of qkd and classical channels over 100-km fiber with 10-dbm classical launch power*, 2023. arXiv: 2304.13828 [quant-ph].

[15] S. Diadamo, B. Qi, G. Miller, R. Kompella, and A. Shabani, "Packet switching in quantum networks: A path to the quantum Internet", *Physical Review Research*, vol. 4, no. 4, p. 043 064, Oct. 2022, ISSN: 26431564. DOI: 10.1103/PHYSREVRESEARCH.4.043064/FIGURES/14/MEDIUM.

[16] J. M. Thomas, G. S. Kanter, and P. Kumar, *Designing noise-robust quantum networks coexisting in the classical fiber infrastructure*, 2023. arXiv: 2304.09076 [quant-ph].

[17] S. J. B. Yoo and P. Kumar, "Quantum wrapper networking", in *2021 IEEE Photonics Conference (IPC)*, IEEE, 2021, pp. 1–2.

[18] S. J. B. Yoo, S. K. Singh, M. B. On, *et al.*, *Quantum wrapper networking*, 2023. arXiv: 2305.00591 [quant-ph].

[19] S. J. B. Yoo, "Optical packet and burst switching technologies for the future photonic Internet", *Journal of Lightwave Technology*, vol. 24, no. 12, pp. 4468–4492, 2006, ISSN: 07338724. DOI: 10.1109/jlt.2006.886060.

[20] M. B. On, S. K. Singh, G. Gul, *et al.*, "Demonstration of quantum channel monitoring via quantum wrappers", in *Optical Fiber Communication Conference (OFC) 2023*, Optica Publishing Group, 2023, Tu3H.4.

[21] S. J. B. Yoo, "Optical-label switching, MPLS, MPLambdaS, and GMPLS", *https://doi.org/10.1117/12.445182*, vol. 4585, pp. 1–11, Oct. 2001, ISSN: 0277786X. DOI: 10.1117/12.445182.

[22] W. M. Mellette, J. Kelley, A. Forencich, and G. C. Papen, "Characterization of Burst-Mode Links for Optical Circuit Switching", *Journal of Lightwave Technology, Vol. 40, Issue 9, pp. 2823-2829*, vol. 40, no. 9, pp. 2823–2829, May 2022. DOI: 10.1364/JLT.40.002823.